Statistical structure of 2D Stokes parameters of birefringent biotissues images

O.V.Angelsky, A.G.Ushenko*, Ye.G.Ushenko, A.O.Angelskaya

Chernivtsi National University, 2 Kotsyubinsky St., 58012 Chernivtsi, Ukraine
*ushenko-bio@itf.cv.ukrtel.net

Received: 30.10.2004

Abstract

The correlation structure of 2D Stokes parameters for physiologically normal and pathologically changed biotissues is studied. The set of diagnostically urgent interconnections between the physiological state of the biotissue and the statistical moments of 2D Stokes parameters is found.

Keywords: Stokes vector, biotissue, tomography, fibril, polarization

PACS: 42.62.-b, 42.62.Be, 42.25.Lc, 42.25.Ja, 81.70.Tx

1. Introduction

Elaboration of modern optical techniques for medical tomography is one of the most important directions in the diagnostics of physiological state of biotissues (BT) [1, 2]. In this respect, optical coherence tomography (OCT) [3 – 7] and its novel branch, polarization-sensitive OCT (PSOCT) [8 - 11], which is based on measuring 2D depth-resolved parameters of the Stokes vector ($2DS_i$) of BT images, have sufficient prospects. They are simple, sensitive enough and error-proof and so enable one to obtain reliable information on the physiological processes.

Analysis of $2DS_i$ may result in important medical information about the microstructure of BT, as well as the values and coordinate distributions of the parameters of optical anisotropy of their architectonic nets, formed by the bundles of collagen, myosin, etc. [12, 13].

Further progress of the PSOCT techniques may be associated with elaborating new methods of analysis and processing of $2DS_i$ and a subsequent search for diagnostically urgent interconnections of their structure and the physiological states of BT.

The present study is directed towards combining the possibilities of PSOCT with statistical, correlation and fractal methods for analysis of 2D parameters of the Stokes vector of the object field, with the purpose of early diagnostics of pre-tumour changes in the connective tissues (CT). The following items represent methodological basis of our investigation:

1. The CT are two-component amorphous-crystalline structures [13], polarization properties of which are described in the most complete way with a superposition of Mueller matrices of their amorphous ($\{a_{ik}\}$) and crystalline ($\{c_{ik}\}$) components.
2. The geometry of the CT architectonics has hierarchical, self-similar structure (microfibrils, fibrils, fascia, fibres, bundles, etc.), which is discrete and characterized with a scaling repetition in the wide range of "optical" sizes (1 – 1000 μm). Structural elements of the CT architectonics hierarchy

manifest the properties of optically uniaxial crystals [14].

As a consequence, the matrix operator of the CT may be written as follows:

$$\{B\}=\begin{Vmatrix} 1 & 0 & 0 & 0 \\ 0 & c_{22}+a_{22} & c_{23} & c_{24} \\ 0 & c_{32} & c_{33}+a_{33} & c_{34} \\ 0 & c_{42} & c_{43} & c_{44}+a_{44} \end{Vmatrix}, \qquad (1)$$

$$\begin{aligned} &a_{22}\approx a_{33}\approx a_{44}=e^{-\tau d},\\ &c_{22}=\cos^2 2\rho+\sin^2 2\rho\cdot\cos\delta;\\ &c_{23}=c_{32}=\cos 2\rho\sin 2\rho(1-\cos\delta),\\ &c_{24}=-c_{42}=-\sin 2\rho\sin\delta;\\ &c_{33}=\sin^2 2\rho+\cos^2 2\rho\cos\delta;\\ &c_{34}=-c_{43}=\cos 2\rho\sin\delta; c_{44}=\cos\delta. \end{aligned} \qquad (2)$$

Here τ denotes the extinction coefficient of the CT layer with the width d, ρ the orientation of fibril packing in the plane of the sample and δ the light phase shift produced by anisotropy of the substance.

The transformation of polarization state of the beam probing the CT is described by the matrix equation

$$\begin{pmatrix} S_1^* \\ S_2^* \\ S_3^* \\ S_4^* \end{pmatrix}=\begin{pmatrix} S_1^0 \\ \{c_{22}S_2^0+c_{23}S_3^0+c_{24}S_4^0\}+\{a_{22}S_2^0\} \\ \{c_{32}S_2^0+c_{33}S_3^0+c_{34}S_4^0\}+\{a_{33}S_3^0\} \\ \{c_{42}S_2^0+c_{43}S_3^0+c_{44}S_4^0\}+\{a_{44}S_4^0\} \end{pmatrix}= \qquad (3)$$

$$=\begin{pmatrix} \mathrm{K}_1 \\ \mathrm{K}_2\left[\rho(X,Y);\delta(X,Y)\right] \\ \mathrm{K}_3\left[\rho(X,Y);\delta(X,Y)\right] \\ \mathrm{K}_4\left[\rho(X,Y);\delta(X,Y)\right] \end{pmatrix}+\begin{pmatrix} \mathrm{A}_1 \\ \mathrm{A}_2 \\ \mathrm{A}_3 \\ \mathrm{A}_4 \end{pmatrix},$$

where S_i^0 and S_i^* are respectively the parameters of Stokes vectors of the illuminating beam and the polarization image of CT. The latter vector represents a superposition of Stokes vectors corresponding to the components, which are homogeneous (A_i) and inhomogeneous (K_i) with respect to the polarization.

It follows from Eqs. (1) – (3) that both the geometric (or orientational, $\rho(X,Y)$) and the optical (or phase, $\delta(X,Y)$) parameters of CT architectonic nets play a crucial role in forming polarization structure of the image. The impact of these two factors in forming a set of 2D distributions $\mathrm{K}_i(X,Y)$ can be regarded as a result of multiplying several coordinate-dependent functions $F_k\left[\rho(X,Y);\delta(X,Y)\right]$, whose explicit form is determined by the polarization state of the probing beam and the set of the matrix elements $\{c_{ik}\}$.

For the sake of simplicity, let us assume that a plane-polarized wave with the azimuth 45° with respect to the inclination surface (i.e., $S^0=\{1;0;1;0\}$) probes the BT. The analysis shows that the above restriction should not violate further conclusions. In this specific case, polarization structure of the CT image is determined by the relations

$$\begin{aligned} \mathrm{K}_2(X,Y)&=\cos 2\rho(X,Y)\sin 2\rho(X,Y)\times\\ &\times\left(1-\cos\delta(X,Y)\right),\\ \mathrm{K}_3(X,Y)&=\sin^2 2\rho(X,Y)+\\ &+\cos^2 2\rho(X,Y)\cos\delta(X,Y),\\ \mathrm{K}_4(X,Y)&=\cos 2\rho(X,Y)\sin\delta(X,Y). \end{aligned} \qquad (4)$$

It is seen from Eq. (4) that the range of changing for the Stokes parameters is extremely wide ($-1.0\le \mathrm{K}_{i=2,3,4}(\rho,\delta)\le 1.0$). This fact proves morphological "sensitivity" of coordinate distributions of the parameters $\mathrm{K}_i\{[\rho(X,Y);\delta(X,Y)]\}$ to the changes in architectonic structure of CT, which, in turn, is connected with physiological state of the latter [14].

For any real CT, the coordinate distributions $[\rho(X,Y);\delta(X,Y)]$ are rather complicated and versatile. They can acquire not only statistical character, but also a fractal one. The last assumption is based on the fact that the mechanism for growing architectonic nets is represented by flat and spatial twist-effects of orientation and scaling transformations of fibrillar components, the analogues of affine transformations forming mathematical fractals [15]. As a result, geometric structures are formed, which are determined by self-similar

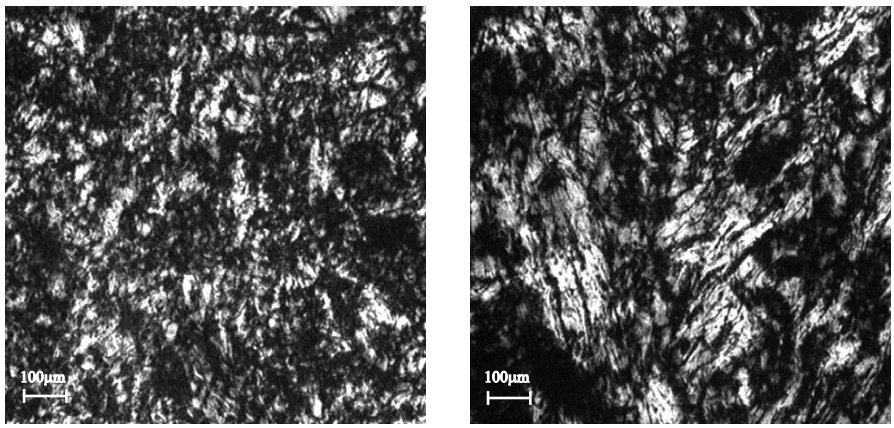

Fig. 1. Images of architectonics of physiologically normal (a) and pathologically changed (b) CT samples obtained in the case of crossed polarizers.

coordinate scale distributions of structural elements, namely their longitudinal ($d(X,Y)$) and transverse sizes and the orientations (or angular directions $\rho(X,Y)$) of fibril packing in the plane of the CT layer under test. Therefore, applying different methods for the analysis of 2D Stokes parameters of the CT images would be relevant, while evaluating comprehensively the geometric structure of the CT architectonics. One of such methods lies in synthesizing the two known approaches in the CT diagnostics (the polarization correlometry [14] and the fractal analysis [15] of their images), resulting in a laser polarization fractalometry of CT. It includes experimental determination of $2DS_i$ set, with the following calculations of (i) statistic moments of the first (M_S), second (D_S) and higher (A_S, E_S) orders of $2DS_i$, (ii) 1D ($C_{X,X}[S_i(X,Y)]$) and 2D ($C_{X,Y}[S_i(X,Y)]$) correlation functions of $2DS_i$, and (iii) fractal dimensions $FD[S_i(X,Y)]$ of the $2DS_i$ set.

2. Characteristics of the objects of investigation

"Optically thin" ($\tau \le 0.1$ cm^{-1} and the geometric thickness d =30 μm – see also [17, 18, 19]) histological sections of physiologically normal and pathologically changed* CT of the uterus cervix were studied. Their parameters are as follows: the absorption coefficient μ_a = 2.2 cm^{-1}, the scattering coefficient μ_s =185 cm^{-1} and the anisotropy parameter g =0.82. The architectonic nets of such the CT are formed by the protein collagen bundles (Fig. 1a and 1b), for which the birefringence is equal to $\Delta n(CT) \approx 1.5 \times 10^{-3}$.

The pathological changes of the CT are morphologically accompanied with the formation of "growth directions" and the increase in the sizes of collagen fibres (see Fig. 1b).

3. Optical Scheme of Investigation

Fig. 2 presents the optical scheme for measuring coordinate distributions of the Stokes vector parameters of the CT images. The CT samples were illuminated by a collimated (∅ = 10^4μm) beam of He-Ne laser (λ = 0.6328 μm). Polarization illuminator consisting of quarter-wave plates 3 and 5 and polarizer 4 formed the following set of polarization states of the illuminating beam: 1 (the incident azimuth 0^0), 2 (90^0), 3 ($+45^0$) and 4 (the right-handed circularly polarized light). Polarization images of the CT were projected onto the plane of light-sensitive area of CCD-camera 10 (800x600 pixels in square), using micro-objective 7. This provided the scale range of 2 – 2000 μm for the studied

* These pathological changes are due to dysplasia, a pre-cancer state of the CT, whose diagnostics is extremely difficult by means of traditional histo-chemical methods [16].

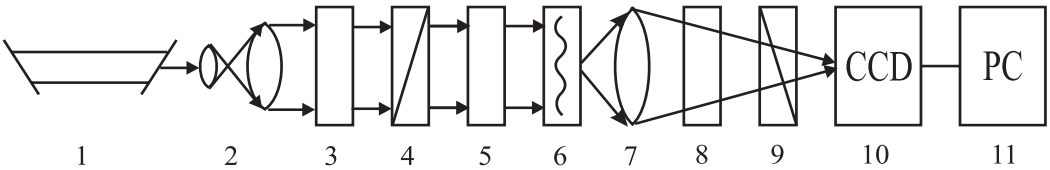

Fig. 2. Experimental setup: 1, He-Ne laser, 2, collimator, 3, 5 and 8, quarter wave plates, 4, polarizer, 9, analyser, 6, sample under test, 7, micro-objective, 10, CCD camera, and 11, personal computer.

structural elements of CT. The conditions of the experiment were chosen so as to eliminate a spatial and angular aperture filtering, while forming the CT images. This was achieved with coordinating the angular characteristics of light scattering indicatrices of the CT samples ($\Omega_{CT} \approx 16^0$, with Ω_{CT} implying the plane angle of the cone, in which 98% of all energy of the scattered light is emitted) and the angular aperture of the micro-objective ($\Delta\omega = 20^0$).

The analysis of CT images was performed with the aid of system including quarter-wave plate 8 and polarizer 9. As a result, the set of partial Stokes vectors, which form $2DS_i$, was determined for every pixel of the CCD camera. The following algorithm was used for this purpose:

$$S_1^* = I_{0^0} + I_{90^0}, S_2^* = I_{0^0} - I_{90^0}, S_3^* = I_{45^0} - I_{-45^0}, S_4^* = I_{\otimes} - I_{\oplus}, \quad (5)$$

where $I_{0^0}, I_{90^0}, I_{\pm 45^0}, I_{\otimes}$ and $I_{\oplus}$ are the light intensities, the subscripts 0^o, 90^o and $\pm 45^o$ denote the azimuths of linearly polarized components and the subscripts $\otimes$ and $\oplus$ – respectively right- and left-handed circularly polarized components of the CT images.

4. Analysis and Discussion of Experimental Data

The results of studies for the set of $2DS_i$ are presented in Fig. 3 and 4 for different types of the CT images. Here, the coordinate

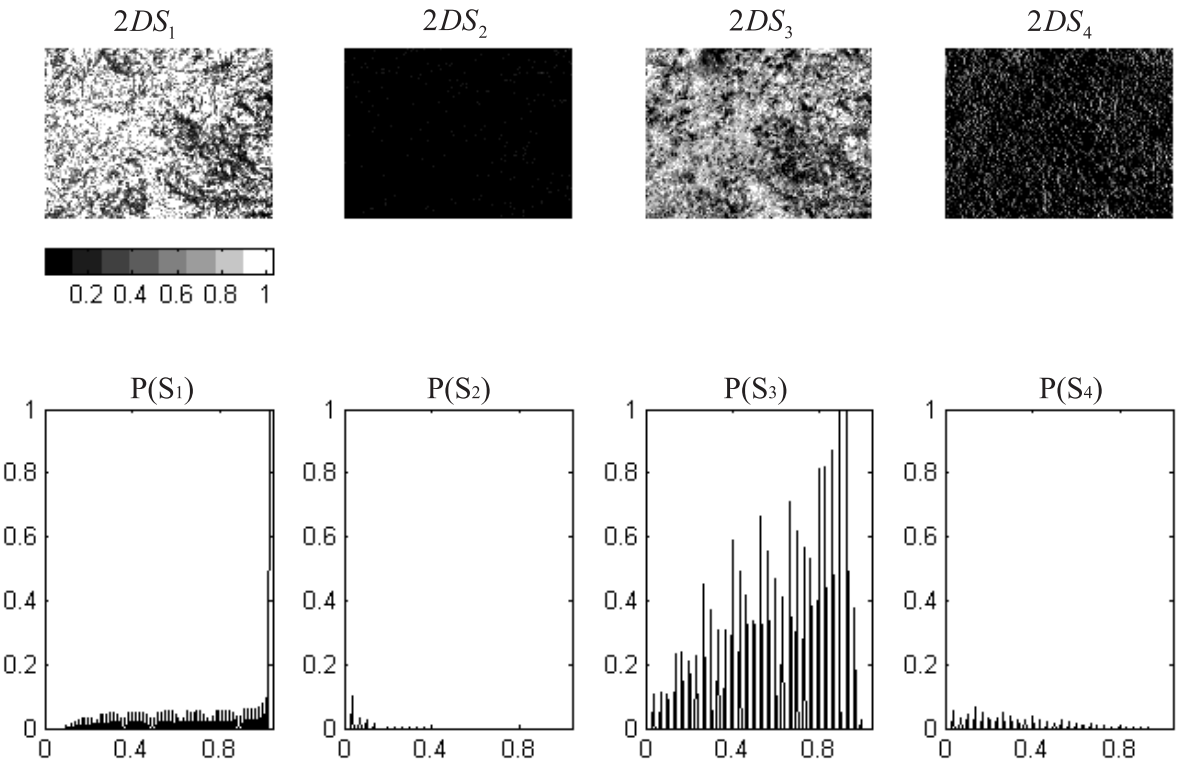

Fig. 3. Coordinate ($2DS_1$, $2DS_2$, $2DS_3$, $2DS_4$) and statistical (P_1, P_2, P_3, P_4) structures of the Stokes vector's polarization parameters describing the image of physiologically normal CT sample.

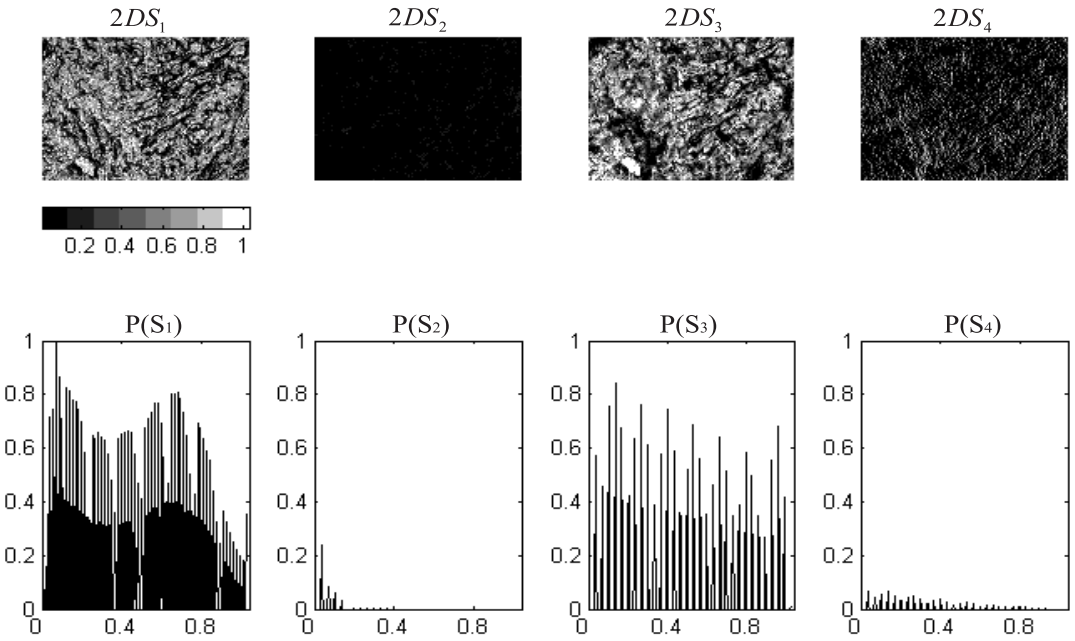

Fig. 4. Coordinate ($2DS_1$, $2DS_2$, $2DS_3$, $2DS_4$) and statistical (P_1, P_2, P_3, P_4) structures of the Stokes vector's polarization parameters describing the image of CT sample with dysplasia.

distributions for the Stokes parameters $2DS_i$ (see the upper row of each figure) and the corresponding probability distributions $P_i\{S_i(X,Y)\}$ (see the lower row) are shown for both physiologically normal (Fig. 3) and pathologically changed (Fig. 4) CT images.

Using the obtained data, one can arrive at the following conclusions:

- the polarization structure of the CT images is inhomogeneous and the set of all $2DS_i$ demonstrates a wide range for the changes of their relative values (from 0.0 to 1.0);
- the coordinate distributions of the relative values of different $2DS_i$ have individual character;
- the probability distributions $P_i\{S_i(X,Y)\}$ represent a "quasi-discrete" structure, consisting of continuous series of local extrema;
- the comparative analysis of the statistic structure of $2DS_i$ for the normal and pathologically changed CT samples proves that the relative values and the size of changing for the ensemble of $2DS_2$ and $2DS_4$ parameters increase in case of the CT images with pre-cancer dysplasia. The contrary trend is observed for the coordinate distributions of the third Stokes vector parameter, $2DS_3$. These differences in polarization characteristics of the CT images of both types are illustrated quantitatively in Table 1, where the statistic moments of $2DS_{i=2,3,4}$ of the first, second and higher orders are compared.

Comparative analysis of the data gathered in Table 1 shows diagnostic sensitivity of the whole set of statistic moments of $2DS_{i=2,3,4}$ of the first, second and higher orders to the physiological state of CT.

Let us analyse those data from the viewpoint of optical model of CT architectonics suggested in this paper. Formation of new "growth directions" and scaling of CT collagen fibre sizes under the conditions of appearance of the pre-tumour state (see Fig. 1b) manifest themselves optically in increasing "phase-shifting ability" (i.e., increasing $\delta(X,Y)$ parameter) of the architectonic net substance. This is why the relative values of the Stokes parameters increase for the images of these samples ($S_i \Rightarrow \begin{cases} \sin\delta \\ 1-\cos\delta \end{cases}$) and decrease in case

Table 1. Statistic characteristics of $2DS_{i=2,3,4}$ Stokes parameters of the CT images.

Parameter	Normal CT (37 samples)		CT with dysplasia (36 samples)		Comparison
$2DS_{i=2}$	M_S	0.01	M_{SP}	0.08	$M_S<M_{SP}$
	D_S	0.0003	D_{SP}	0.02	$D_S<D_{SP}$
	A_S	4.56	A_{SP}	39.73	$A_S<A_{SP}$
	E_S	136.3	E_{SP}	1174.5	$E_S<E_{SP}$
$2DS_{i=3}$	M_S	0.57	M_S	0.19	$M_S>M_{SP}$
	D_S	0.06	D_{SP}	0.01	$D_S>D_{SP}$
	A_S	60.7	A_{SP}	533.4	$A_S<A_{SP}$
	E_S	198.6	E_{SP}	956.7	$E_S<E_{SP}$
$2DS_{i=4}$	M_S	0.13	M_{SP}	0.23	$M_S<M_{SP}$
	D_S	0.04	D_{SP}	0.09	$D_S<D_{SP}$
	A_S	4.2	A_{SP}	45.9	$A_S<A_{SP}$
	E_S	282	E_{SP}	2030.1	$E_S<E_{SP}$

of the normal state ($S_i \Rightarrow \cos\delta$). In our experimental situation (see Eqs. (4)) $S_{i=2,4}$ and $S_{i=3}$ are the respective examples. Therefore, for their coordinate distributions we observe the increase in the average ($M_{S2,4}$) and the dispersion ($D_{S2,4}$) of the ensemble of relative Stokes parameter values in case of physiologically normal CT, and vice versa for the parameters M_{S3} and D_{S3}.

The correlation functions $C_{X,Y}\left[S_i(X,Y)\right]$ give some additional information on the coordinate distribution of $2DS_{i=2,3,4}$ related to the changes in orientation structure of architectonics in the plane of the CT layer. Fig.5 presents 1D "sections" $C_{X,X}\left[S_i(X,Y)\right]$ of autocorrelation functions (ACF) of the Stokes parameters $2DS_{i=2,3,4}$ for the images of physiologically normal (see the upper row) and

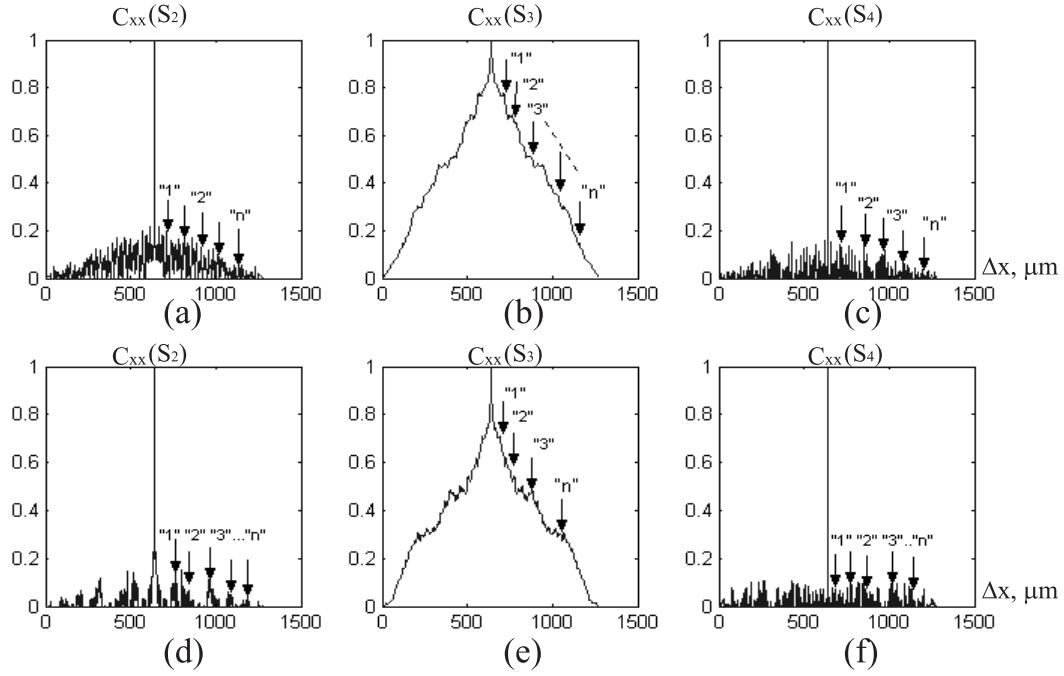

Fig. 5. Set of the ACF for the Stokes vector's polarization parameters ($2DS_2$, $2DS_3$ and $2DS_4$) of the images of physiologically normal (a, b and c) and pathologically changed (d, e and f) CT samples. Δx is the step for the 2D distributions of the Stokes vector parameters, which is equal to 1 pixel in our calculations.

pathologically changed (the lower row) CT. The results obtained prove the following:

- the ACF of 2D distributions of the Stokes parameters for the whole set of CT images represents a convolution of monotonously decreasing (non-correlated) and "quasi-periodic" (correlated) components. We mean that the latter is represented by a series of local extrema of $C_{X,X}\left[S_i(X,Y)\right]$ ("1", "2",…, "n" – see Fig. 5a, 5b and 5c), whose spatial frequencies and amplitudes are associated with self-similarity of packing and scales of the collagen fibres, which form the CT architectonics;
- the processes of forming new "growth directions" of the architectonic fibres in the pathologically changed CT images are accompanied with increasing quantity and amplitudes of the correlation peaks for the ACF of 2D distributions of the Stokes parameters (see Fig. 5d, 5e and 5f).

Thus, the correlation component of all $C_{X,X}\left[S_{i=2,3,4}(X,Y)\right]$ dependences appears to be "sensitive" to both the orientation and the phase-shift changes in the architectonics of the CT samples under study. On the other hand, quantitative estimation of such the changes would be difficult due to small amplitudes of the correlation peaks, when compare with the principal correlation maximum of the ACF. Calculating the dispersion D_{Pj} of the extrema values for the power spectra of the corresponding ACF $W_j\left\{C_{X,X}\left[S_{i=2,3,4}(X,Y)\right]\right\}$ appears to be a more convenient way. Those parameters are depicted in Fig. 6. Finally, statistically averaged D_{Pj} parameters found for the groups of physiologically normal and pathologically changed tissues are presented in Table 2. One can see that the appearance of dysplasia is accompanied with a sufficient increase in the dispersion of power spectra for all of the Stokes vector parameters describing the optical CT images.

Thus, the polarization-correlation analysis for coordinate distributions of the Stokes vector parameters of CT images has shown that the use of the parameter D_{Pi} would be promising for diagnostics of orientation changes in the fibrillar structure of their architectonic nets.

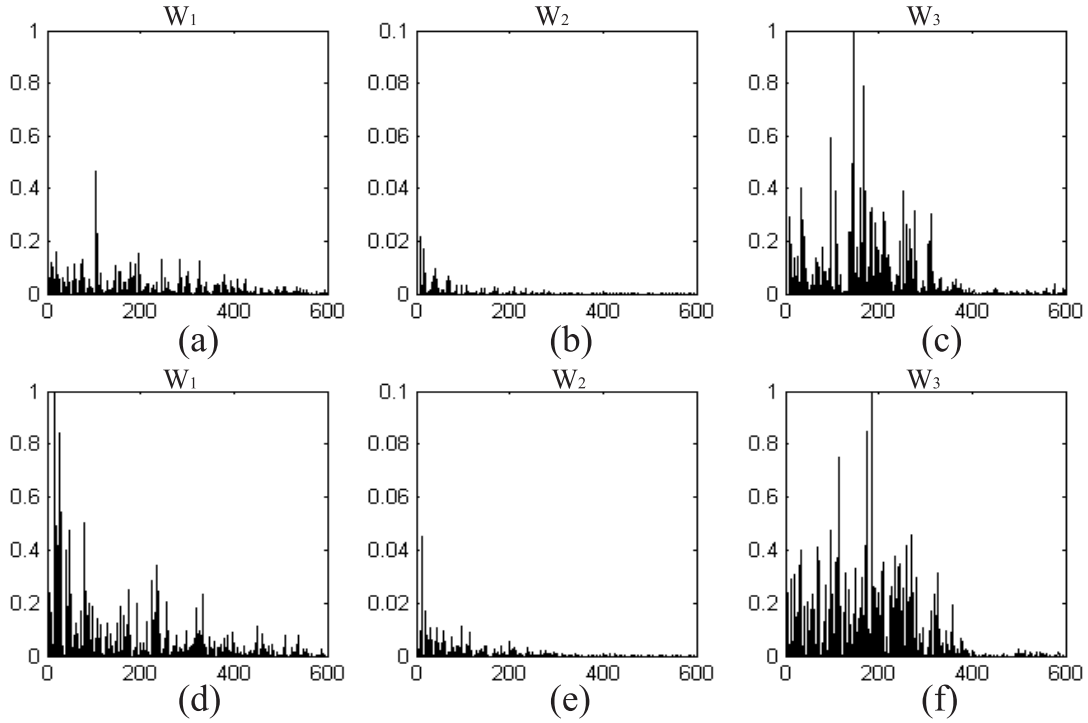

Fig. 6. Spectral densities W_i of the Stokes vector's polarization parameters $2DS_2$, $2DS_3$ and $2DS_4$ of the images of physiologically normal (a, b and c) and pathologically changed (d, e and f) CT samples.

Table 2. Dispersion of the extrema for the ACF power spectra for $2DS_i$ parameters.

Parameters		CT	
$P_j\{\mathrm{K}_{X,X}[S_{i=2,3,4}(X,Y)]\}$		Physiologically normal	Pathologically changed
$P_2\{\mathbf{K}_{X,X}[S_{i=2}]\}$	D_{P2}	0.11	0.24
$P_3\{\mathbf{K}_{X,X}[S_{i=3}]\}$	D_{P3}	0.21	0.33
$P_4\{\mathbf{K}_{X,X}[S_{i=4}]\}$	D_{P4}	0.09	0.17

5. Conclusions

1. Polarization fractalometry of $2DS_i$ parameters of the BT images' Stokes vector has turned out to be efficient for diagnosing changes in the coordinate distributions of the orientations and optical anisotropy of their architectonic nets formed by the collagen bundles.

2. The set of diagnostically urgent properties is established, which determine the interconnections between the statistic, correlation and fractal characteristics of $2DS_i$ parameters of the BT images and the physiological state of the BT.

3. The processes of pathological changes in the BT architectonics manifest themselves in the following:

- the changes in the values of the first and second statistic moments of $2DS_i$ (respectively, the increase for $2DS_{i=2,4}$ and the decrease for $2DS_{i=3}$);
- the increase, by an order of magnitude, in the third and fourth statistic moments of the Stokes vector parameters;
- the increase in the dispersion D_{Pj} characterising the power spectra extrema for the ACF of $2DS_i$.

References

1. D. Huang, E. A. Swanson, C. P. Lin, J. S. Schuman, W. G. Stinson, W. Chang, M. R. Hee, T. Flotte, K. Gregory, C. A. Puliafito, J. G. Fujimoto, Science **254** (1991) 1178-1181.
2. A.F. Fercher, J. Biomed. Opt. **1** (1996) 157-173.
3. W. S. Bickel and W. M. Bailey, Amer. J. Phys. **53** (1995) 468-478.
4. J. F. de Boer, S. M. Srinivas, B. H. Park, T. H. Pham, Z. Chen, T. E. Milner, J. S. Nelson, IEEE J. Sel. Top. Quant. Electron. **5** (1999) 1200-1203.
5. J. F. de Boer, T. E. Milner, M. J. C. van Gemert, and J. S. Nelson, Opt. Lett. **22** (1997) 934-936.
6. J. F. de Boer, S. M. Srinivas, A. Malekafzali, Z. Chen, and J. S.Nelson, Opt. Express **3** (1998) 212–218.
7. J. F. de Boer, T. E. Milner, and J. S. Nelson, Opt. Lett. **24** (1999) 300–302.
8. G. Yao and L.-H. Wang, Opt. Lett. **24** (1999) 537-539.
9. S.-L. Jiao, G. Yao, and L.-H. Wang, Appl. Opt., **39** (2000) 6318-6324.
10. S. Jiao and L.-H. Wang, Opt. Lett. **27** (2), (2002) 101–103.
11. S. Jiao, W. Yu, G. Stoica, and L.-H. Wang, Opt. Lett., **28** (14), (2003) 1206-1208.
12. J. M. Schmitt and S. H. Xiang, Opt. Lett. **23** (1998) 1060–1062.
13. S.C.Cowin, J. Biomed. Eng., **122** (2000) 553-568.
14. A.G.Ushenko, Laser Physics, **10** (6), (2000) 1-7.
15. O.V.Angelsky, D.N.Burcovets, A.V.Kovalchuk, and S.T.Hanson, Appl. Opt. **41** (22) (2002) 4620-4629.
16. "Pathology of Both Vagina and Cervix of Uterus" / Ed. V.I. Krasnopolskiy. – Moscow: Medicine, (1997) 124-136. (in Russian).
17. S.L.Jacques, C.A.Alter and S.A.Prahl, Lasers Life Sci. **1** (1987) 309-333.
18. R.Marchesini, A.Bertoni, S.Andreola and A.Dogariu, Appl. Opt. **28** (1989) 2318-2324.
19. Y.P.Zhao, C.F.Cheng, G.C.Wang, and T.M.Lu, Surf. Sci. Lett. **409** (1998) L703-L708.